Eur. Phys. J. Plus (2021) 136:995
https://doi.org/10.1140/epjp/s13360-021-01971-2

THE EUROPEAN PHYSICAL JOURNAL PLUS

Regular Article

Simulation of an active interrogation system for the interdiction of special nuclear materials

Anderson V. S. Alves[1,a], **Francesco d'Errico**[1,2,3]

[1] School of Medicine, Yale University, New Haven, CT, USA
[2] Scuola di Ingegneria, Università di Pisa, and Istituto Nazionale di Fisica Nucleare, Sezione di Pisa, Pisa, Italy
[3] Yale Center for Emergency Preparedness and Disaster Response, New Haven, CT, USA

Received: 10 January 2021 / Accepted: 18 September 2021

Abstract Special nuclear materials hidden in shipping containers are extremely difficult to detect through their faint spontaneous emission of neutrons and photons. R&D efforts focus on active interrogation techniques, employing external beams of neutrons or high-energy X-rays to first trigger fission reactions and then detect prompt or delayed neutrons and/or photons. Our group created an active interrogation system based on detectors developed by Yale University and the University of Pisa. These detectors contain liquid droplets that vaporize when exposed to fast neutrons, but are insensitive to X-rays. The system was tested with an X-ray generator based on a 9 MeV electron LINAC available at an active interrogation facility. Copper is used as an X-ray production target at this facility, which prevents the production of photo-neutrons. With this system, we detected a sample of natural uranium either uncovered or shielded under heavy loads of wood or steel pipes. In order to interpret the experimental results, the response of our detector systems was assessed using Monte Carlo simulations with the code PHITS. Computational results are in good agreement with the experimental ones and open the way to simulations of real-world scenarios of interest to nonproliferation and homeland security, namely active interrogation at a standoff.

1 Introduction

Combating terrorism is one of the highest priorities, and a key aspect of this effort is preventing special nuclear material from being introduced into the country, hidden in the large containers entering through shipping ports and carrying the large majority of cargo. The possible presence in these containers of weapon components containing special nuclear materials is extremely difficult to detect through their faint radioactive signature. While radiation emitted by Pu-239 may be picked up by high-sensitivity devices, that of highly-enriched U-235 (HEU) is virtually impossible to detect with passive interrogation techniques. In fact, the emission consists of an extremely low yield of neutrons and a weak emission of low-energy gamma rays which are strongly attenuated by surrounding materials. For these reasons, active interrogation (AI) techniques, whereby an external beam of neutrons or high-energy x-rays is

[a] e-mail: anderson.ks.alves@gmail.com (corresponding author)

Published online: 04 October 2021

typically used to trigger fission reactions, are considered the only viable option to detect the presence of HEU. These techniques are also effective in the detection of Pu-239, as illustrated in a comprehensive DOE Report [6] and the review by Slaughter et al. [8].

Among the favored active interrogation approaches is using X-rays from 9 MV electron linear accelerators. These X-rays have an effective energy causing adequate photofission in SNM, while avoiding neutron production in most 'innocent' materials, such as shipping container structures and legitimate contents. An exception is the production of photo-neutrons in naturally occurring deuterium; these neutrons can reach 3 MeV when produced by 9 MV X-rays. A critical element in the implementation of the approach is the development and characterization of the detector technology. Indeed, the interdiction of SNM also places heavy performance requirements on the detector systems. In order to record the intense prompt neutron emission, an ideal detector should not only discriminate X-rays but also neutrons below ~ 3 MeV. Since the scan must be acquired and evaluated in real time, the detectors must be active and offer a rate-insensitive readout. Superheated emulsions satisfy these requirements and have been used to develop detector systems for active interrogation purposes. This work describes the Monte Carlo simulations that were performed to examine and fully interpret the results of some active interrogation measurements of shielded special nuclear material with superheated emulsions.

2 Methodology

To simulate an Active Interrogation System (AIS), we used the general-purpose Monte Carlo code PHITS v3.25 [10], which is capable of dealing with multipurpose simulations by dividing the physical processes into two categories, transport and collision processes. A 9 MV X-ray source is used to generate photonuclear reactions in special nuclear materials. Photofission neutrons that cross the selected region of interest are then detected, and their flux and energy distribution can be tallied. The Monte Carlo simulations of neutrons penetrating through the material are a compilation of the individual neutrons' histories from the point of entrance in a certain material to either its absorption or transmission [11]. A history is terminated when the neutron is absorbed or no longer satisfies predetermined scoring criteria; hence, neutrons are tracked until they are either absorbed, fall below certain threshold energy, or leave the material or region of interest.

In recent versions, PHITS adopted the Japanese Evaluated Nuclear Data Library (JENDL) Photonuclear Data File 2004 (JENDL/PD-2004) to determine the total cross-section for photonuclear reactions [9]. The Evaluated Nuclear Data Format (ENDF) library, in particular the recently released ENDF/B-VIII.0 [5], was added to the model for a cross-section comparison analysis. All simulations in this work used 300 K as default temperature. Our simulations also use the Intra-Nuclear Cascade of Liège (INCL) and KUROTAMA models. The INCL model [12] simulates nuclear reactions induced by nucleons and other particles at intermediate energies, while the KUROTAMA model defines nucleon-nucleus reaction cross-sections [13].

In our approach, at least 1×10^{10} histories of photons emitted from the source were simulated per setup. To address statistical uncertainties, we biased the neutron flux generated from the photo-nuclear reactions against the photo-atomic interactions by adding the *pnimul* parameter that controls the photonuclear cross-sections [10]. This also greatly reduces the computation times. We used track tallies to measure the flux of neutrons going through each region of interest. All PHITS results presented in this paper have statistical uncertainties below 10% (at one relative standard deviation level).

Table 1 Properties of the materials used in the simulations

Material	Density (g/cm^3)	Elemental fractions (%)						
		H	C	N	O	Fe	Si	Other
Wood-plank crate	0.40	6.0	50.0	1.0	43.0	0.0	0.0	0.0
Steel-pipe crate	0.65	0.0	0.2	0.0	0.0	98.7	0.0	1.1
Steel platform	7.85	0.0	0.2	0.0	0.0	98.7	0.0	1.1
Concrete	2.30	1.0	0.1	0.0	52.9	1.4	33.7	10.9
Plastic case	0.90	7.5	75.0	17.5	0.0	0.0	0.0	0.0

2.1 Geometry

Our simulation implemented a geometry based on the Passport Systems facility [2]. Experimental measurements at this facility had been previously conducted [d'Errico F., Martin J.D., Alves A.V.S., Chierici A., D'Olympia N., Wilson C., Korbly, S. Active interrogation of shielded special nuclear material with superheated emulsions. Manuscript in preparation (2021)], and the obtained results are compared to the simulated ones. The setup comprises the high-energy X-ray source, steel sliding platform, concrete floor and walls, a sample of special nuclear material (SNM), i.e., a natural uranium disk, the shielding materials, i.e., two crates containing wood (1 m^3 and 0.40 g/cm^3) and steel pipes (1 m^3 and 0.65 g/cm^3), and a plastic case containing the cylinder with dimensions and composition similar to those of superheated emulsion modules inside their carry-on case [3]. The density and elemental fractions of the materials used are summarized in Table 1.

Three configurations were simulated: The first is the uncovered uranium disk being irradiated, and the second and third setups represent the disk being shielded by the steel-pipe crate and wood-plank crate placed on top, respectively. The superheated emulsion detector regions were defined as two sections of a cylinder shell centered at the uranium disk, with heights equal to the superheated emulsion detector (20 cm). The shell radius is equal to 212 cm, and the total distance between the uranium disk and the detectors is 220 cm, as shown in Fig. 2. The region is centered on the uranium disk with the same radius in the three setups. This is done to further reduce the computing time while still being realistic with the size of the superheated emulsion detector. Two square regions of 120×120 cm^2 are also defined as representative of the scintillators panels that were present at the Passport Systems facility. Those scintillator regions are used to compare their tallied flux with our superheated emulsion detector.

2.2 Source

The source is simulated as a 9 MV X-ray parallel beam with a cross section of 30×120 cm^2. This area spans the crates used for shielding and the uranium disk. The X-ray spectrum we implemented is shown in Fig. 3. To reduce the computation time, energy cutoffs for photons below 2.2 MeV and neutrons below 0.1 MeV were later applied in our simulations. This energy threshold was used to preserve the photonuclear reactions that occur on deuterium, mainly in the wood shielded setup.

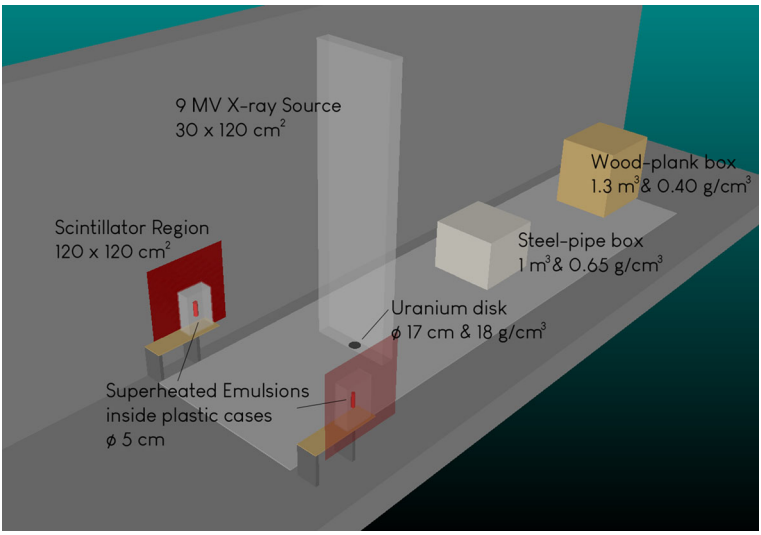

Fig. 1 Geometry of the unshielded uranium disk irradiation setup

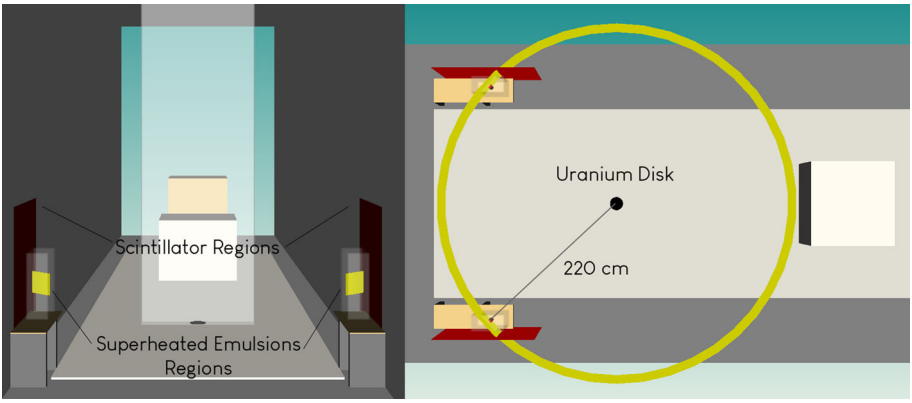

Fig. 2 Selected regions of detection for both the scintillators and superheated emulsions

3 Results and discussion

3.1 Generated photofission neutrons

To visually assess the generation of photofission neutrons, tracks were tallied with a limited number of histories, equal in each geometry, using 2×10^9 histories of photons per setup. Besides the neutron cutoff at 0.1 MeV, neutrons below 3.0 MeV were excluded from the final flux tally. This is the threshold provided by superheated emulsions and it is chosen mainly to discriminate the neutrons generated in photonuclear reactions on the deuterium nuclei of wood and other organic materials. In practice, this energy selection in the superheated emulsions is introduced by controlling the pressure inside the detector [4]. The difference between the tracks produced with and without this energy selection can be seen in Fig. 4.

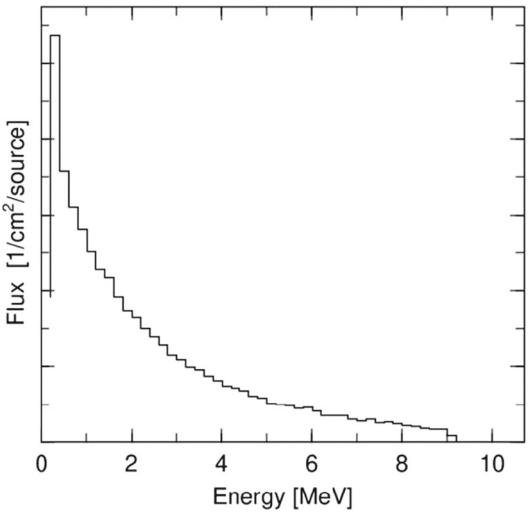

Fig. 3. 9 MV X-ray source spectra before the cutoff is applied

The total number of neutrons generated with the wood crate covering and shielding the uranium disk is greatly increased by the photonuclear reactions in the wood itself due to the above-mentioned small, but non-negligible, amount of deuterium. However, due to the presence of hydrogen in the wood, a higher attenuation occurs of neutrons generated in the uranium disk, compared to the other geometries. These factors cause a smaller neutron flux at the region of interest.

A comparison between the PHITS default JENDL/PD-2004 nuclear library and an added ENDF/B-VIII.0 library was performed by simulating the same unshielded uranium disk setup. The obtained neutron fluence ration between JENDL and ENDF was 1.19. This result suggests that, for the energy range between 3 and 10 MeV used in our simulations, the JENDL library has a higher overall cross-section for photo fission reactions, generating a higher number of neutrons than the ENDF library.

3.2 Neutron flux

The overall neutron flux at the region of interest is shown in Fig. 5, where the values of both superheated emulsions regions were averaged. Results conformed the expected behavior for the wood shielded geometry, as it shows a lower number of neutrons reaching the detector region.

By selecting the energy of the neutrons (>3 MeV), we can verify their tallied flux and calculate the ratios between each shielding setup. In Table 2, the neutron flux detected by the superheated emulsions in the experimental setup at the Passport Systems facility is compared with the flux tallied in the PHITS simulations.

From the data comparison in Table 2, we can observe an excellent agreement between experimental and simulated results. These ratios confirm that, with a simplified but accurate geometry, we were able to achieve a result close to the actual experimental data.

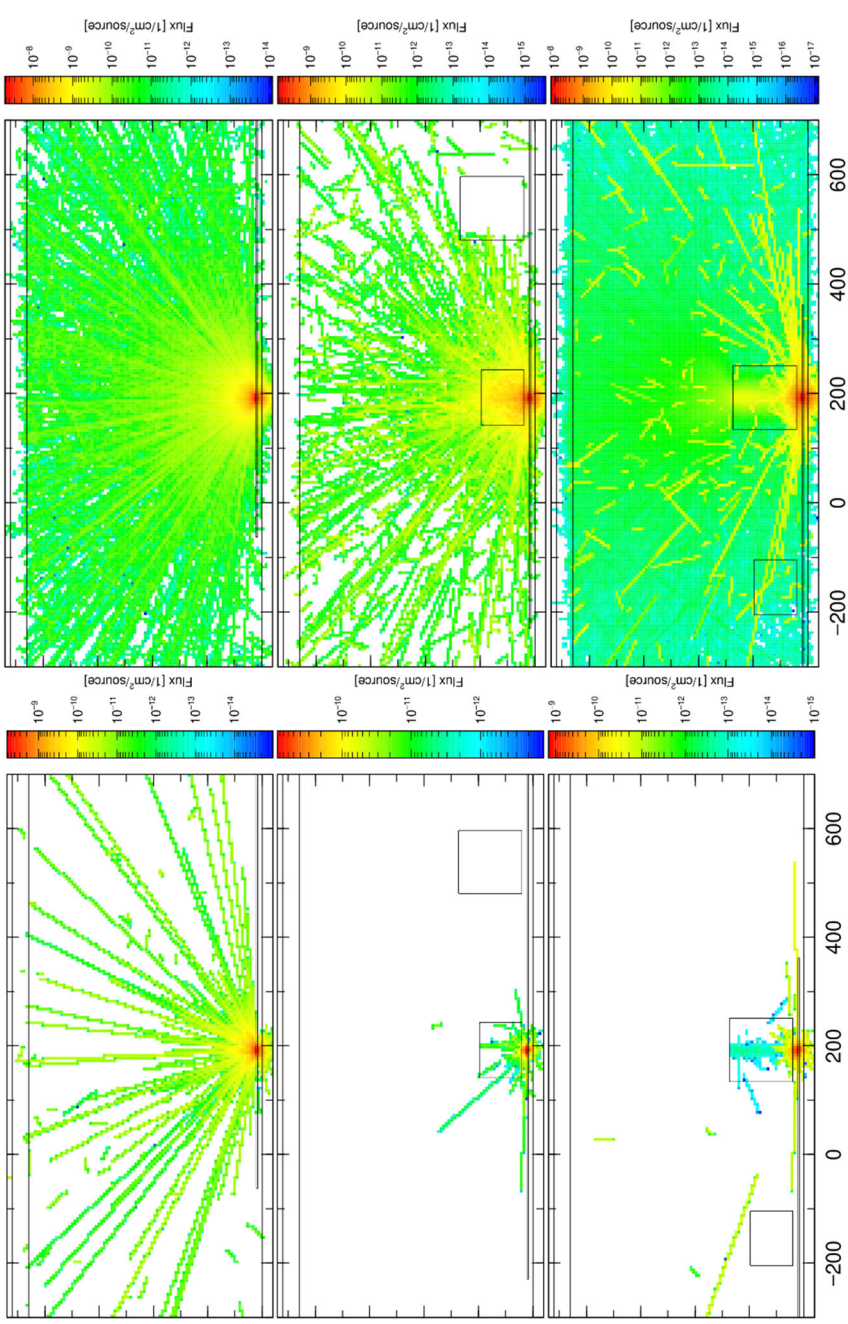

Fig. 4 Photofission generated neutrons with a cutoff on 3 MeV (left) without cutoff (right) at the three setups: no shielding, steel box, and wood box, respectively, from top to bottom

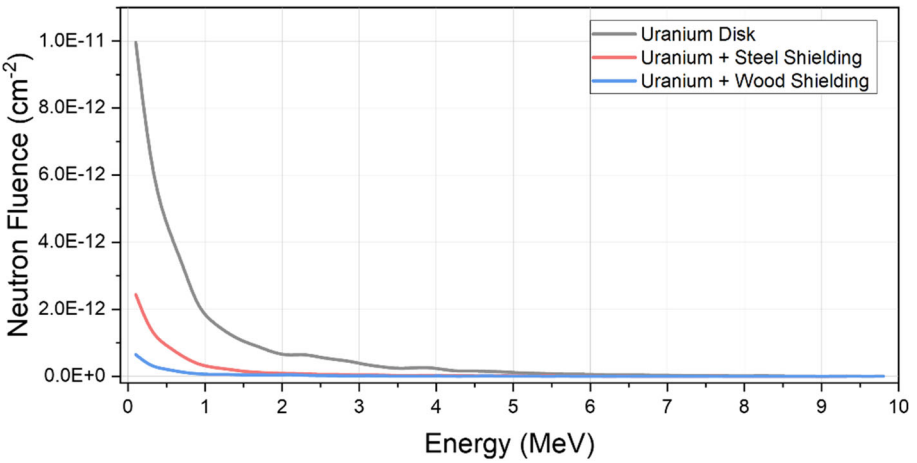

Fig. 5 Obtained neutron flux in the region of detection. The three setups are represented: black (no shielding), red (steel-pipe crate), and blue (wood-plank crate)

Table 2 Neutron flux ratio for the unshielded and shielded setups obtained for the superheated emulsions in experimental analysis and the PHITS calculated tally for the regions of detection

Ratio of counts for different configurations	Experimental data (d'Errico et al., 2021)	PHITS simulated data
U/(U + Steel)	7.0	$7.97 \pm 6\%$
U/(U + Wood)	20.5	$22.59 \pm 8\%$

4 Conclusions

In this work, we simulated a complete active interrogation system, including source, shielded SNM, and detectors, and we obtained computational results in good agreement with the experimental ones. This agreement opens the way to simulations of real-world scenarios of interest to non-proliferation and homeland security, namely active interrogation at standoff. Complex systems are currently being simulated such as the model developed at PNNL of a LINAC coupled with a large cargo vehicle loaded with containers filled with a variety of items [7]. Materials of disparate densities, hydrogen content, and atomic numbers, such as air, polyethylene, and concrete will be considered and modeled. As a part of these simulations, we will also resume studies of the possibility of using multiple detector thresholds in order to recognize fission neutrons against photoneutrons from (α,n) or (γ,n) sources [[1]].

Acknowledgements This research was supported in part by DHS Grant 2016-DN-077-ARI107.

References

1. R.E. Apfel, F. d'Errico, J.D. Martin, Fast discrimination of neutrons from (□-n) and fission sources. Radiat. Prot. Dosim. **70**(1–4), 113–116 (1997)

2. A. Danagoulian, W. Bertozzi, C.L. Hicks, A.V. Klimenko, S.E. Korbly, R.J. Ledoux, C.M. Wilson, Prompt neutrons from photofission and its use in homeland security applications. In: IEEE International Conference on Technologies for Homeland Security (HST), Waltham, MA, 379–384 (2010)
3. F. d'Errico, A. Fulvio, Superheated emulsions for the detection of special nuclear material. Radiat. Meas. **46**, 1690–1693 (2011)
4. F. d'Errico, G. Felici, A. Chierici, R. Zagarella, Detection of special nuclear material with a transportable active interrogation system. Eur. Phys. J. Plus **133**, 451–460 (2018)
5. F. d'Errico, A. Chierici, M. Gattas-Sethi, S. Philippe, R. Goldston, A. Glaser, New developments and applications of superheated emulsions: warhead verification and special nuclear material interdiction. Radiat. Prot. Dosimetry. **180**(1–4), 210–214 (2018)
6. DOE, Report on the Workshop on the Role of the Nuclear Physics Research Community in Combating Terrorism. DOE/SC-0062 (2002).
7. S.M. Robinson, R. Kouzes, R.J. McConn Jr, R. Pagh, J. E. Schweppe, E.R. Siciliano, Creation of Realistic Radiation Transport Models of Radiation Portal Monitors for Homeland Security Purposes. In: 2005 IEEE Nuclear Science Symposium Conference Record. 1014–1018 (2005)
8. D. Slaughter, M. Accatino, A. Bernstein, J. Candy, A. Dougan, J. Hall, A. Loshak, D. Manatt, A. Meyer, B. Pohl, S. Prussin, W. Walling, D. Weirup, Detection of special nuclear material in cargo containers using neutron interrogation LLNL Report UCRL-ID-155315 (2003)
9. S. Noda, S. Hashimoto, T. Sato, T. Fukahori, S. Chiba, K. Niita, Improvement of photonuclear reaction model below 140 MeV in the PHITS code. J. Nucl. Sci. Technol. **52**(1), 57–62 (2015)
10. T. Sato, Y. Iwamoto, S. Hashimoto, T. Ogawa, T. Furuta, S. Abe, T. Kai, P.-E. Tsai, N. Matsuda, H. Iwase, H. Shigyo, L. Sihver, K. Niita, Features of particle and heavy ion transport code system (PHITS) version 3.02. J. Nucl. Sci. Technol. **55**, 684–690 (2018)
11. S.F. Olukotun, S.T. Gbenu, O.F. Oladejo, F.O. Balogun, M.I. Sayyed, S.M. Tajudin, E.I. Obiajunwa, M.K. Fasasi, The effect of incorporated recycled low density polyethylene (LDPE) on the fast neutron shielding behaviour (FNSB) of clay matrix using MCNP and PHITS Monte Carlo codes. Radiat. Phys. Chem. **182**, 109351 (2021). https://doi.org/10.1016/j.radphyschem.2021.109351
12. A. Boudard, J. Cugnon, J.-C. David, S. Leray, D. Mancusi, New potentialities of the Liège intranuclear cascade model for reactions induced by nucleons and light charged particles. Phys. Rev. C. **87**, 014606 (2013)
13. K. Iida, A. Kohama, K. Oyamatsu, Formula for proton-nucleus reaction cross section at intermediate energies and its application. J. Phys. Soc. Japan **76**, 044201 (2007)